of the five galls with micropterous adults present ($\chi^2 = 4.95$, $P = 0.026$). These data demonstrate that *Koptothrips* kill *Oncothrips* and vice versa. A direct defensive role for micropterous adults of *O. habrus*, protecting the foundress, is suggested by the finding that the foundress was dead in all six of the galls without micropterous adults (where the *Koptothrips* was always alive), but she was dead in only two (40%) of the five galls with micropterous adults present ($\chi^2 = 4.95$, $P = 0.026$). Moreover, in these two galls with dead foundresses the micropterous adults were all dead ($n = 3$ in one gall, 8 in the other) or moribund ($n = 1$).

Do micropterous adults show a higher propensity than foundresses to attack invaders? Experimental removal of the first few adults that emerged from a hole in the gall, or attacked *Koptothrips* held at the hole, showed that in *O. habrus* micropterous females emerged from the gall and attacked *Koptothrips* with a higher probability than did foundresses (Table 1). By contrast, in *O. tepperi*, which exhibits less dimorphism in foreleg size than *O. habrus* (Fig. 1), foundresses and micropterous females did not differ significantly in tendency to emerge from the gall. In both species, micropterous males sometimes emerged or attacked invaders. Altruism by male haploids is not expected under inclusive fitness theory, unless the cost-to-benefit ratio for the selfish alternative is extremely high.

The observations and experiments described above indicate that micropterious adults of *O. tepperi* and *O. habrus* represent 'soldiers', defined as individuals morphologically or behaviourally specialized for defence. Soldiers are also found in aphids[7], termites[1] and a polyembryonic wasp[8], and in each of these taxa the soldiers are more or less sterile and the taxa are regarded as eusocial[3]. Do *O. tepperi* and *O. habrus* also exhibit eusociality?

Eusociality is normally defined by the presence of three traits: (1) overlap in generations between parents and their offspring; (2) cooperative brood care; and (3) reproductive division of labour, "with more or less sterile individuals working on behalf of fecund individuals"[1]. In *O. tepperi* and *O. habrus*, the adult lives of the foundress and her micropterous offspring overlap substantially, and micropterous adults, by defending the gall and their gall-mates in an often self-sacrificing manner, are clearly engaging in cooperative brood care. Differences in reproduction between foundresses and micropterous females were analysed by dissecting females and ranking the size of their largest oocyte from one (undeveloped ovaries) to five (chorionated eggs). Many micropterous females had developing oocytes in both *O. tepperi* (67% of 273) and *O. habrus* (58% of 154), and some micropterous females contained fully developed chorionated eggs (12% of 273 in *O. tepperi*; 7% of 154 in *O. habrus*). But in both species micropterous females had significantly smaller oocytes on average than did foundresses (paired *t*-tests comparing foundresses with the mean for micropterous females, two samples for each species; $t = 2.94$, 3.81, $P = 0.005$, 0.0012, $n = 39$, 20 for *O.tepperi*; $t = 8.82$, 8.71, $P < 0.0001$ for each, $n = 20$, 10 for *O. habrus*). Determining whether or not micropterous females have lower lifetime direct reproduction than foundresses would require analysis of maternity within complete adult broods. Similarity of reproductive rates is, however, highly unlikely because the offspring of the foundress alone, as micropterous adults and larvae, fill the gall almost completely: there is simply insufficient space in the gall for micropterous females to produce as many adult offspring as do foundresses.

The morphological specialization, defensive behaviour, and reduced reproduction of micropterous adults of *O. tepperi* and *O. habrus* indicate that these two species are eusocial. What selective pressures might have promoted eusociality among gall thrips in general, and in *O. tepperi* and *O. habrus* in particular? As in eusocial aphids[7], naked mole-rats[3], and many termites[1], gall thips live and feed inside a highly valuable, persistent habitat that they have created, and this habitat is defensible primarily by individuals specialized with weaponry and behaviour for heroic acts[3]. As in eusocial Hymenoptera, female gall thrips can facultatively bias the sex allocation ratio towards females[4,9], produce males by parthenogenesis[9], and exhibit relatednesses to sisters of over one-half, all of which are presumed to favour the origin of eusocial behaviour[10,11]. In *O. tepperi*, broods of macropterous adults are highly female-biased, and in both species, micropterous females in some galls are probably producing only sons as there are no micropterous males present with whom they could mate. Determining the importance of haplodiploidy in the origin and evolution of gall thrips eusociality requires further analysis of genetic relatedness and sex allocation ratios in eusocial and non-eusocial species. □

Received 29 June; accepted 8 September 1992.

1. Wilson, E. O. *The Insect Societies* (Belknap, Harvard Univ. Press, Cambridge, 1971).
2. Andersson, M. *A. Rev. ecol. Syst.* **15,** 165–189 (1984).
3. Alexander, R. D., Noonan, K. & Crespi, B. J. in *The Biology of the Naked Mole-Rat* (eds Sherman, P., Jarvis, J. U. M. & Alexander, R. D.) 3–44 (Princeton Univ. Press, New Jersey, 1991).
4. Crespi, B. J. *J. nat. Hist.* (in the press).
5. Mound, L. A. *Bull. Br. Mus. nat. Hist. (Ent.)* **25,** 389–466 (1971).
6. Mound, L. A. *Ent. Mon. Mag.* **105,** 159–162 (1970).
7. Aoki, S. in *Animal Societies: Theories and Facts* (eds Itô, Y., Brown, J. L. & Kikkawa, J.) 53–65 (Japan Sci. Soc. Tokyo, 1987).
8. Cruz, Y. P. *Nature* **294,** 446–447 (1981).
9. Crespi, B. J. in *Evolution and Diversity of Sex Ratio in Insects and Mites* (eds Wrensch, D. & Ebbert, M.) (Chapman and Hall, New York, in the press).
10. Hamilton, W. D. *J. theor. Biol.* **7,** 1–52 (1964).
11. Trivers, R. L. & Hare, H. *Science* **191,** 249–263 (1976).

ACKNOWLEDGEMENTS. I thank the National Geographic Society for funding this research; R. H. Crozier and members of his laboratory for providing a friendly logistical base; E. Nielsen and I. Naumann of CSIRO Entomology for help with fieldwork; I. Clarke, G. C. Eickwort, C. D. Michener, L. A. Mound and L. Vawter for correspondence and discussion; and W. D. Hamilton, U. Mueller and P. W. Sherman for comments on the manuscript.

# Wing bone stresses in free flying bats and the evolution of skeletal design for flight

**Sharon M. Swartz*, Michael B. Bennett† & David R. Carrier***

* Program in Ecology and Evolutionary Biology, Brown University, Providence, Rhode Island 02912, USA
† Department of Anatomical Sciences, The University of Queensland, Brisbane 4072, Australia

**THE primary mechanical functions of limb bones are to resist deformation, and hence provide stiff levers against which muscles can act, and to be sufficiently strong to prevent breaking under static or dynamic loads which arise from normal and accidental activities[1]. If bones perform these functions with a minimum amount of material, the energetic costs associated with building, maintaining and transporting the skeleton will be minimized[2]. Appropriate skeletal architecture for minimizing mass while maximizing strength depends on forces imposed on structural elements. In the evolutionary acquisition of flight in the bat lineage, the forelimb skeleton must have come to experience locomotor-forces that differed from those engendered by the terrestrial locomotion of non-flying bat relatives. Here we successfully measure *in vivo* strain on the wing bones of flying mammals. Our data demonstrate that torsion and shear are unique and crucial features of skeletal biomechanics during flight, and suggest that the evolution of skeletal design in bats and other flying vertebrates may be driven by the need to resist these loads.**

In typical mammalian locomotion, bones experience repetitive impacts in which forces are closely aligned to the limb's axis. In contrast, during flight, wing muscle contraction and pressure gradients applied by the wing membranes during the generation of lift and thrust apply forces to the long, slender

TABLE 1 Mean maximum peak principle strains magnitudes ($\mu\varepsilon$) and their orientations

| Humerus | Strain | | | | | |
|---|---|---|---|---|---|---|
| | Dorsal | | Ventral | | Medial | |
| | Magnitude | Orientation | Magnitude | Orientation | Magnitude | Orientation |
| Mid-downstroke | 1,554 (83) | 21° (2) | 1,496 (46) | 22° (1) | 2,004 (49) | 21° (0) |
| Bottom of downstroke | 1,188 (37) | 31° (1) | 988 (32) | 21° (3) | 1,852 (45) | 22° (2) |
| Top of upstroke | 488 (23) | 0° (5) | 572 (22) | 2° (2) | 468 (21) | 25° (1) |
| Radius | Dorsal | | Dorsolateral | | Ventral | |
| | Magnitude | Orientation | Magnitude | Orientation | Magnitude | Orientation |
| Mid-downstroke | −1,808 (108) | 28° (1) | −2,184 (47) | 32° (1) | 1,275 (44) | 32° (1) |
| Bottom of downstroke | −2,109 (95) | 27° (1) | −1,912 (60) | 32° (1) | 1,316 (23) | 29° (1) |
| Top of upstroke | −405 (58) | 29° (3) | 904 (40) | 21° (2) | 243 (37) | −10° (3) |

| Humerus | Stress | | | | | | | | |
|---|---|---|---|---|---|---|---|---|---|
| | Dorsal | | | Ventral | | | Medial | | |
| | Longitudinal | Transverse | Shear | Longitudinal | Transverse | Shear | Longitudinal | Transverse | Shear |
| Mid-downstroke | 15.5 (0.9) | −6.8 (1.0) | 4.2 (0.3) | 14.4 (0.5) | −5.5 (0.2) | 10.5 (0.5) | 30.2 (1.0) | −3.0 (0.5) | 15.7 (0.7) |
| Bottom of downstroke | −9.1 (0.8) | 10.8 (0.9) | 10.9 (0.8) | 12.0 (0.4) | −4.1 (0.1) | 5.2 (0.2) | 28.3 (1.1) | 6.2 (0.7) | 10.7 (0.6) |
| Radius | Dorsal | | | Dorsolateral | | | Ventral | | |
| | Longitudinal | Transverse | Shear | Longitudinal | Transverse | Shear | Longitudinal | Transverse | Shear |
| Mid-downstroke | −36.1 (0.7) | 6.8 (0.7) | −8.5 (0.7) | −45.8 (0.6) | −2.1 (0.1) | −11.2 (0.3) | 20.6 (1.2) | −7.9 (0.7) | 5.7 (0.2) |
| Bottom of downstroke | −37.8 (0.9) | 2.2 (0.8) | −8.4 (0.8) | −36.6 (0.9) | −1.7 (0.1) | −7.7 (0.2) | 17.7 (0.6) | −6.0 (0.8) | 2.1 (0.4) |

Each value represents the mean for 2–4 animals over 50 to 119 wingbeats; standard errors follow means in parentheses. Tensile strains are positive and compressive strains are negative. Mean magnitude of stresses (MPa) alon the bones' primary material axes for the high stress (mid-downstroke and bottom of downstroke) portions of the wingbeat cycle. Calculations based on transversely orthotropic model for material characteristics of mammalian compact cortical bone[4].

wing bones, and this complex force distribution changes dynamically throughout the wingbeat cycle[3]. Because of the many unknowns in the mechanical loading on the wings, it is impossible to make accurate and detailed predictions concerning the nature of strains experienced by wing bones during flight. To assess bone loading directly, we carried out the first successful study of natural patterns of bone deformation during free flight in large bats. We surgically implanted rosette strain gauges on the dorsal, ventral and medial or dorsolateral midshaft surfaces of the humerus and radius of four wild-caught grey-headed flying foxes (*Pteropus poliocephalus*; 500–850 g) (Fig. 1). We characterized bone loading throughout the wingbeat cycle by calculating principal strain magnitudes and their orientations to each bone's longitudinal axis, and coordinated these recordings with simultaneous video records of the bats' movements. Bone stresses were then calculated using a transversely orthotropic model for compact bone mechanical properties[4], with the assumption that the material characteristics of cortical bone of large bats is similar to that of birds and other mammals.

Strains recorded from each bone indicate complex loading regimes. Principal strain profiles for each recording site show a triphasic pattern, with peak loads occurring at the middle of the downstroke, the bottom of the downstroke and the top of the upstroke. Between these peaks, strain magnitudes drop considerably, approaching zero during the upstroke (Fig. 2). Peak strain magnitudes (Table 1) are somewhat lower than those

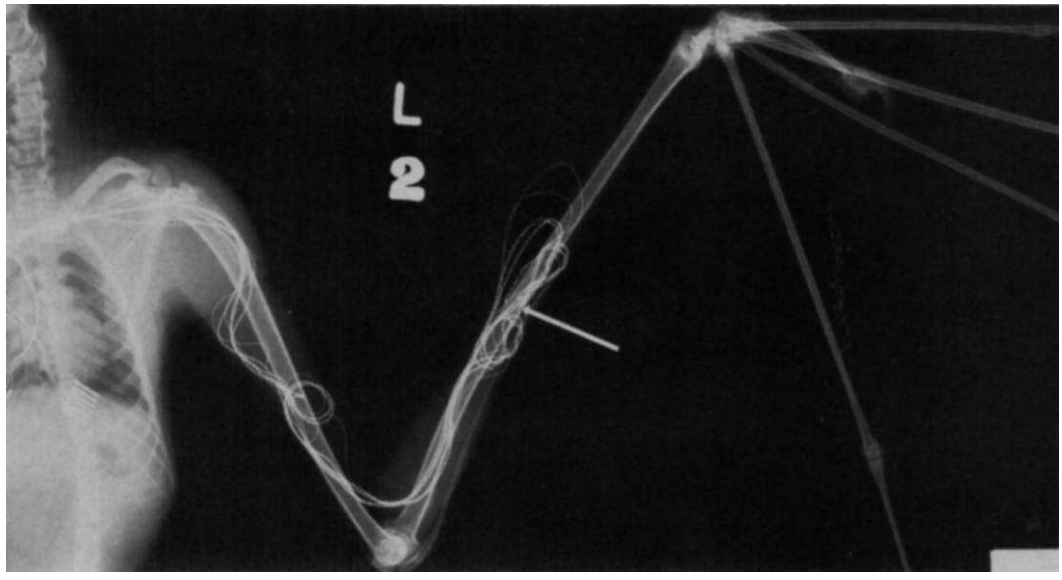


FIG. 1 Radiograph of grey-headed flying fox wing (L2 indicates left wing, subject number 2) implanted with strain gauges. We mist-netted all subjects at the Veterinary Science Farm of the University of Queensland, Brisbane, Australia; they were trained to fly the length of an outdoor flight cage (30 × 2 × 2 m) without stopping. Small rosette strain gauges (Tokyo Sokki Kenkyujo Co. FRA-1) were attached with a self-catalysing cyanoacrylate adhesive to the dorsal, ventral, and dorsolateral or medial midshaft cortices of the right humerus and left radius, as near as possible to midshaft but in areas free of direct muscle attachment to minimize localized distortions in overall bone strain due to muscle pull. The procedure was similar to that previously described[9,18]. Gauge wires were subcutaneously passed proximally from the forearm or arm, ventrally in front of the shoulder, externalized through the skin superficial to the sternum, and soldered to connectors; sufficient slack was left to permit large amplitude wing movements without pulling gauges off the bones. After post-operative recovery, 6–10 channels of strain data were amplified (MicroMeasurements Model 2120AK strain gauge conditioner/amplifiers) and sampled simultaneously at 250–400 Hz on a Macintosh IIfx computer (using National Instruments LabVIEW 2 data acquisition software and a National Instruments NB-MIO-16XL-18 A/D board) by means of a light-weight cable as each bat flew the length of the flight cage.

recorded from terrestrial mammals during vigorous locomotor activities (60–85% of previously observed values)[5–7]. Peak principle strains at mid-downstroke and the bottom of downstroke are oriented at a substantial angle to the bone's long axis, with overall mean orientations of 23° for the humerus and 30° for the radius (orientation of 0° is aligned with the bone's axis, and positive deviations indicate the principal strain axis is rotated in a clockwise direction, with the axis extending along a proximomedial to distolateral direction with the limb in natural flight posture). In keeping with an earlier theoretical model of strength of wing bones in birds in relation to their function to resist aerodynamic forces during flight[8], this pattern of off-axis strain of similar magnitude around the bone circumference is suggestive of significant torsional loading. Similar torsional loading has recently been observed in studies of the pigeon humerus during flapping flight (A. A. Biewener and K. P. Dial, personal communication).

Longitudinal stresses calculated from the raw strain data (Table 1; Fig. 3) are comparable in magnitude to stresses developed in other mammals during fast canters, gallops and some jumps[9–11]. Transverse stresses are large, particularly at the bottom of the downstroke, reaching in the humerus and radius respectively, maxima of 47% and 38% of the longitudinal value during the mid-downstroke and 119% and 34% at the bottom of the downstroke. Shear stresses are also significantly greater in bats than in other mammals (more than 15 MPa, compared with values of no greater than 6 MPa recorded during walking and running in human and dogs[4,12]). These large transverse and shear stresses are both consistent with substantial torsional loads. These results differ significantly from the typical pattern of mammalian limb bone loading, in which bending predominates and torsion is of relatively little significance[13]. This is notable given that bone fails at far lower stress in shear (corresponding to about 65 MPa) than in tension or compression (corresponding to about 150 and 200 MPa respectively)[14].

The mechanism that is most likely to be responsible for producing these torsional stresses in bat wing bones is probably one that is common to all vertebrates capable of active, powered flight. Because the skeleton is near the wing's leading edge in bats, as in all flying vertebrates, the wing's centre of pressure, at which the aerodynamic forces generated during flight act, lies posterior to the major bony supports. Upwardly directed forces at the centre of pressure thus exert a torsional moment in the pronating direction, transmitted through the wing membrane

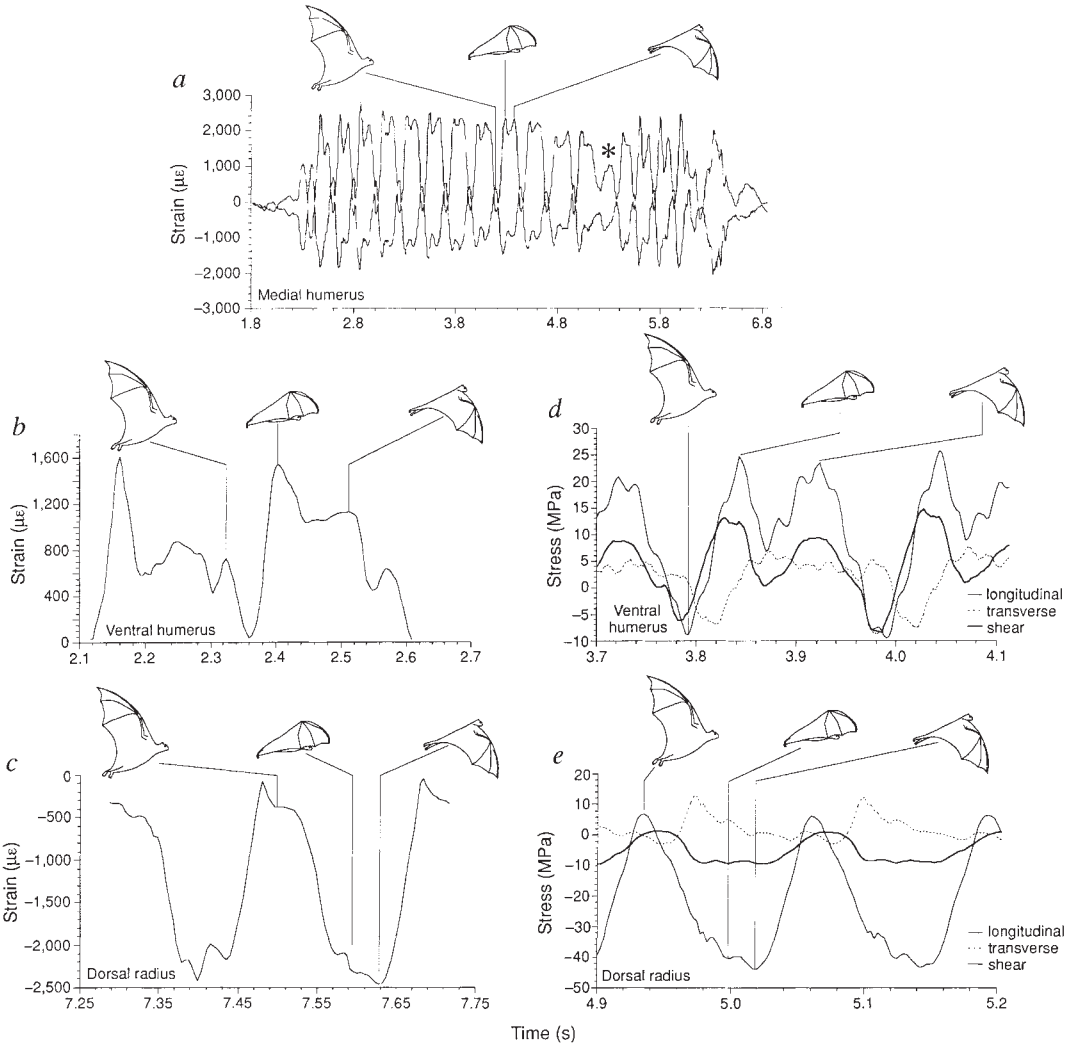


FIG. 2 *a*, Representative maximum and minimum principal strain records from the medial humerus; *b*, maximum principal strain records from ventral humerus and *c*, dorsal radius, and *d*, calculated longitudinal, transverse and shear stresses from the ventral humerus and *e*, dorsal radius of one bat for single flights, correlated with flight kinematics based on videotapes (60 frames per second) taken during recordings. Strain magnitudes are reported in microstrain (change in length/original length × $10^{-6}$); tensile (elongating) strains are positive and compressive (shortening) strains are negative. Stress values in megapascals (MPa) are calculated from raw strain data assuming that material characteristics of bat bone are comparable to those of other mammals and using a transversely orthotropic model for bone stiffness[4]. In *a*, a complete flight sequence is depicted from takeoff (small peaks at the far left), through a number of regular wingbeat cycles, through a postural shift in preparation for landing (asterisk), followed by 5 decelerating wingbeats and landing. In *b*–*e*, maximum principal strains and stresses in the bone's material axes are shown for two representative wingbeats. In *a*, *b* and *c*, magnitude changes continually throughout the locomotor cycle for each recording site; representative mid-downstroke, bottom of downstroke and top of upstroke phases of one wingbeat are indicated by the schematics. Bone strains typically reach their greatest absolute values at mid-downstroke and return to smaller peak values at the bottom of the downstroke and again at the top of the upstroke. Strain values return close to zero during some phases of the locomotor cycle. Peaks in longitudinal stress correspond to those in principal strain; transverse and shear stress peaks may occur at somewhat different points in the wingbeat cycle.

and the extended digits, particularly digits 4 and 5 (ref. 8). In the case of birds, wing feathers may serve the same stress transmission role in a somewhat different fashion. A similar mechanism may be responsible for large transverse stresses, as the stresses in the taut wing are transmitted by means of the attachments of the wing membrane along each bone diaphysis.

The cross-sectional geometry of bat wing bones can be related directly to the need to resist torsional stresses imposed by propulsive downstroke movements. The ability of a beam-like structure to resist torsion depends on the magnitude of torque applied ($T$), the moment arm of the torsional force ($r$), and the polar second moment of area of the beam cross-section ($J$) such that the torsion stress ($\tau$) is $\tau = Tr/J$, where $J$ is $J = \pi(R^4 - r^4)/2$. For a given cross-sectional area, $J$ is maximized by circular cross-sectional geometry of maximum outer diameter and minimum wall thickness.

Bats ought, therefore, to have wider, thinner-walled forelimb bones than terrestrial mammals. Our measurements indicate that the wing bones from which we recorded strains indicative of torsion are indeed thinner-walled than those of other mammals (Fig. 3). It has been previously noted that birds and pterosaurs have thin-walled wing bones[15], with pterosaurs displaying especially marked cortical reduction in the metacarpals.

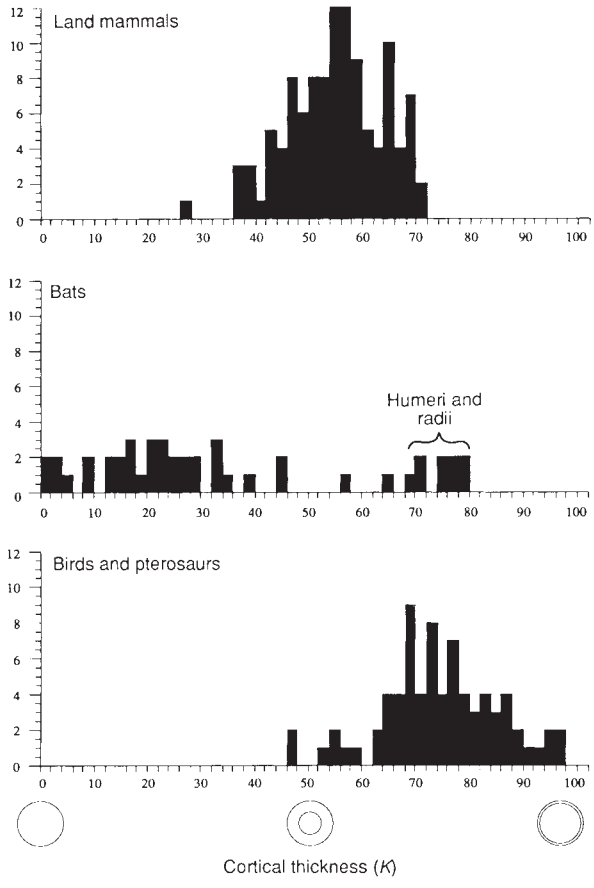


FIG. 3 Frequency distribution of cortical bone thickness for a variety of vertebrates (terrestrial mammal, bird and pterosaur data from ref. 12, additional bat data collected from radiographs of this study's subjects). Cortical thickness is expressed as $K$, and if $R$ is the radius of the bone cross-section, then the marrow cavity thickness equals $KR$ (after ref. 12). When $K$ is zero the bone cross-section is solid, and $K$ approaches 1 as wall thickness approaches zero. Distributions for land mammals and birds plus pterosaurs show some overlap but are clearly distinct, with larger mean $K$ values for flying vertebrates. Bats are clearly distinct from other mammals; the humeri and radii investigated here show reduced thickness compared with other mammals and fall well within the bird/pterosaur range. Other bat wing bones (metacarpals and phalanges) also deviate from the typical mammalian pattern, with greatly increased cortical thickness.

Although this geometrical specialization is typically attributed to the need to reduce skeletal mass in flying animals[16], the skeleton makes up a comparable proportion of total body mass in birds and mammals[17], indicating that other factors are probably involved. We propose that the 'hollow' geometry of bird and pterosaur bones relates directly to an adaptive maximization of $J$ to minimize torsional stress transmitted through wing membranes. Bats have converged upon the bird and pterosaur pattern, with cortical thickness values falling well within the range of birds and pterosaurs and only barely overlapping other mammals. Hence, reduction in thickness in cortical bone in vertebrate wings has evolved at least three times independently, and this fundamental aspect of skeletal design in limbs of flying vertebrates should be interpreted not only as a mechanism to reduce weight but, at least as importantly, as an adaptation to resist large torsional stresses. □

Received 20 July; accepted 8 September 1992.

1. Alexander, R. M. Ker, R. F. & Bennett, M. B. *J. Zool., Lond.* **222,** 471–478 (1990).
2. Alexander, R. M. *Sci. Prog., Oxf.* **67,** 109–130 (1981).
3. Rayner, J. M. V. in *Recent Advances in the Study of Bats* (eds Fenton, M. B., Racey, P. & Rayner, J. V. M.) 23–42 (Cambridge Univ. Press, UK, 1987).
4. Carter, D. R. *J. Biomech.* **11,** 199–202 (1978).
5. Biewener, A. A. & Taylor, C. R. *J. exp. Biol.* **123,** 383–400 (1986).
6. Biewener, A. A., Swartz, S. M. & Bertram, J. E. A. *Calc. Tiss. Int.* **39,** 390–395 (1986).
7. Rubin, C. T. & Lanyon, L. E. *J. theor. Biol.* **107,** 321–327 (1984).
8. Pennycuick, C. J. *J. exp. Biol.* **46,** 219–233 (1967).
9. Biewener, A. A., Thomason, J. & Lanyon, L. E. *J. Zool., Lond.* **201,** 67–82 (1983).
10. Biewener, A. A., Thomason, J. & Lanyon, L. E. *J. Zool., Lond.* **214,** 547–565 (1988).
11. Rubin, C. T. & Lanyon, L. E. *J. exp. Biol.* **101,** 187–212 (1982).
13. Bertram, J. E. A. & Biewener, A. A. *J. theor. Biol.* **131,** 75–92 (1988).
14. Nordin, M. & Frankel, V. H. in *Basic Biomechanics of the Musculoskeletal System* (eds Nordin, M. & Frankel, V. H.) 3–29 (Lea & Febiger, Philadelphia and London, 1989).
15. Currey, J. D. & Alexander, R. M. *J. Zool. Lond.* **206,** 453–468 (1985).
16. Pough, F. H., Heiser, J. B. & McFarland, W. N. *Vertebrate Life* (Macmillan, New York, 1985).
17. Prange, H. D., Anderson, J. F. & Rahn, H. *Am. Nat.* **113,** 103–122 (1979).
18. Lanyon, L. E. *Acta orthop. belg.* **42,** 98–108 (1976).

# Positive selection of T-lymphocytes induced by intrathymic injection of a thymic epithelial cell line

**Stanislav Vukmanović*, Andres G. Grandea III*, Susan J. Faas†, Barbara B. Knowles† & Michael J. Bevan***

* Department of Immunology and Howard Hughes Medical Institute, University of Washington, Seattle, Washington 98195, USA
† The Wistar Institute of Anatomy and Biology and University of Pennsylvania, Philadelphia, Pennsylvania 19104, USA

**T LYMPHOCYTES recognize antigens as peptide fragments associated with molecules encoded by the major histocompatibility complex (MHC) and expressed on the surface of antigen-presenting cells[1]. In the thymus, T cells bearing $\alpha\beta$ receptors that react with the MHC molecules expressed by radioresistant stromal elements are positively selected for maturation[2–5]. In (A × B → A) bone marrow chimaeras, T cells restricted to the MHC-A haplotype are positively selected, whereas MHC-B-reactive thymocytes are not. We investigated whether the introduction of particular thymic stromal elements bearing MHC-B molecules could alter the fate of B-reactive T cells in these (A × B → A) chimaeras. Thymic epithelial cell (TEC) lines expressing H-2$^b$ were introduced by intrathymic injection into (H-2$^{b/s}$ → H2$^s$) bone marrow chimaeras and we measured their ability to generate H-2$^b$-restricted cytotoxic T-lymphocytes (CTLs). We report here that one TEC line, 427.1, was able positively to select CTLs specific for influenza and vesicular stomatitis virus antigens in association with class I H-2$^b$ molecules. In addition, line 427.1 can process cytoplasmic proteins**